Inorg. Chem. **2004**, *43*, 2895–2905

pH-Specific Synthesis of a Dinuclear Vanadium(V)–Peroxo–Citrate Complex in Aqueous Solutions: pH-Dependent Linkage, Spectroscopic and Structural Correlations with Other Aqueous Vanadium(V)–Peroxo–Citrate and Non-Peroxo Species

M. Kaliva,[†] C. P. Raptopoulou,[‡] A. Terzis,[‡] and A. Salifoglou*[,†]

Department of Chemistry, University of Crete, Heraklion 71409, Greece, and Institute of Materials Science, NCSR "Demokritos", Aghia Paraskevi 15310, Attiki, Greece

Received March 15, 2003

Aqueous reactions of V_2O_5 or VCl_3 in the presence of the physiological citric acid and hydrogen peroxide, in a pH specific fashion, afforded a new vanadium(V)–peroxo–citrate material isolated in a pure crystalline form. Elemental analysis pointed to the molecular formulation $(NH_4)_6[V^V_2O_2(O_2)_2(C_6H_4O_7)_2]\cdot 4.5H_2O$ (**1**). Complex **1** was further characterized by UV–vis, FT-IR, and X-ray crystallography. Compound **1** crystallizes in the monoclinic space group *C*2/*c* with $a = 12.391(5)$ Å, $b = 15.737(7)$ Å, $c = 17.102(7)$ Å, $\beta = 110.84(1)°$, $V = 3117(1)$ Å^3, and $Z = 4$. The structure of the anionic assembly consists of a planar $V^V_2O_2$ core with two fully deprotonated citrates bound to it through the central carboxylate and alkoxide moieties as well as one of the terminal carboxylate groups. The presence of one peroxide group attached to each vanadium(V) renders the geometry around each metal center pentagonal bipyramidal. Key structural and spectroscopic features of **1** correlate with those seen in the peroxo congener and low-pH analogue $(NH_4)_2[V^V_2O_2(O_2)_2(C_6H_6O_7)_2]\cdot 2H_2O$ (**3**), in which all terminal carboxylate groups are protonated. In solution, simple pH-dependent transformation of **1** to **3** attests to their participation in the requisite speciation and potentiates the presence of other similar peroxo analogues not yet isolated and characterized. The reactivity of **1** through transformation reactions, yielding a plethora of well-characterized species, establishes a linkage among various species with the same or different vanadium oxidation states. Collectively, the data reflect soluble forms of vanadium with peroxide and citrate that contribute to the requisite pH-dependent distribution of that metal ion and likely influence biological processes.

Introduction

The presence of vanadium in abiotic as well biotic systems has been amply established over the years.[1] Focus on the specific area of vanadium biochemistry and its potential biological role(s) stems from that element's presence in the active sites of biological systems,[2] especially the metalloenzyme systems haloperoxidases[3] and alternative nitrogenases.[4] Equally important, however, appear to be vanadium's multiple and complex roles as inorganic cofactor, sustaining diverse physiological activities in lower and higher organisms, including humans. Most notable among such

* To whom correspondence should be addressed. E-mail: salif@chemistry.uoc.gr. Phone: +30-2810-393-652. Fax: +30-2810-393-601.
[†] University of Crete.
[‡] NCSR "Demokritos".

(1) (a) Baran, E. J. *J. Inorg. Biochem.* **2000**, *80*, 1−10. (b) Rehder, D. *Biometals* **1992**, *5*, 3−12. (c) Zubieta, J. *Comments Inorg. Chem.* **1994**, *3*, 153−183. (d) Chen, Q.; Salta, J.; Zubieta, J. *Inorg. Chem.* **1993**, *32*, 4485−4486. (e) Rehder, D. *Angew. Chem., Int. Ed. Engl.* **1991**, *30*, 148−167. (f) Wever, R.; Kustin, K. In *Advances in Inorganic Chemistry: Vanadium, a Biologically Relevant Element*; Sykes, A. G., Ed.; Academic Press: New York, 1990; Vol. 35, pp 103−137.

(2) (a) Bayer, E. In *Metal Ions in Biological Systems: Amavadin, the Vanadium Compound of Amanitae*; Sigel, H., Sigel, A., Eds.; Marcel Dekker: New York, 1995; Vol. 31, Chapter 12, pp 407−421. (b) Smith, M. J.; Ryan, D. E.; Nakanishi, K.; Frank, P.; Hodgson, K. O. In *Metal Ions in Biological Systems: Vanadium in Ascidians and the Chemistry in Tunichromes*; Sigel, H., Sigel, A., Eds.; Marcel Dekker: New York, 1995; Vol. 31, Chapter 13, pp 423−490. (c) Fraústo da Silva, J. J. R. *Chem. Speciation Bioavailability* **1989**, *1*, 139−150.

(3) (a) Weyand, M.; Hecht, H.; Kiess, M.; Liaud, M.; Vilter, H.; Schomburg, D. *J. Mol. Biol.* **1999**, *293*, 595−611. (b) Vilter, H. In *Metal Ions in Biological Systems: Vanadium and its Role in Life*; Sigel, H., Sigel, A., Eds.; Marcel Dekker: New York, 1995; Vol. 31, Chapter 10, pp 325−362. (c) Butler, A. *Curr. Opin. Chem. Biol.* **1998,** *2*, 279−285.

(4) Liang, J.; Madden, M.; Shah, V. K.; Burris, R. H. *Biochemistry* **1990**, *29*, 8577−8581.

10.1021/ic034283i CCC: $27.50 © 2004 American Chemical Society
Published on Web 03/30/2004

activities are its antitumorigenicity,[5] mitogenicity,[6] and inhibition of key metabolic enzymes such as phosphoglucomutases and others.[7] Outstanding among the various effects that vanadium can exert is its ability to promote insulin mimetic activity in the pathophysiological state of diabetes mellitus in humans.[8−10]

The wide spectrum of activities exhibited by vanadium undoubtedly arises as a result of complex interactions of the metal ion in its predominant oxidation states +4 and +5 with a plethora of high molecular as well as low molecular mass biomolecules. Of the low molecular mass bioligands interacting with vanadium are carboxylic acids, representative of which is citric acid. The latter organic substrate is present in human plasma at high concentration (0.1 mM),[11] thus being capable of promoting interactions with various metal ions, like vanadium, potentially modulating a plethora of metabolic functions.

On the basis of the aforementioned attributes of vanadium interactions with biomolecules, it becomes essential that (a) bioavailable species be fully defined in the aqueous media where pertinent vanadium interactions take place, (b) soluble species be identified, and ultimately (c) the nature and chemical and structural properties of those species be explored as they constitute the basis on which potential biochemical activity is promoted at the biological level. Key to unravelling this bewildering riddle is the aqueous structural speciation of vanadium in the presence of organic metal ion binder(s) like citric acid. To this end, solution speciation studies[12,13] undertaken in the past had suggested the presence of vanadium(IV,V) complexes with citrate as well as other biologically relevant ligands. Subsequent synthetic efforts revealed a number of dinuclear vanadium−citrate species of variable structural and spectroscopic properties.[14−16] On the other hand, no information exists to date on the aqueous speciation of ternary systems involving vanadium with citric acid in the presence of the physiological agent hydrogen peroxide. Equally scarce is also the presence of synthetically isolated and characterized complexes of vanadium(V) with citric acid and hydrogen peroxide. It is worth noting that vanadium−peroxo species have been shown to exert insulin mimetic activity in addition to the previously reported antitumorigenic activity in in vitro experiments.

In view of the significance of the above-mentioned (bio)chemistry, we have embarked on synthetic efforts targeting aqueous vanadium−peroxo−citrate complexes. Herein, we report on (a) the synthetic approaches, the isolation, and spectroscopic and structural characterization of a new aqueous vanadium−peroxo−citrate complex near physiological pH values; (b) the pH dependent acid−base and thermally induced transformations surrounding its chemical reactivity; and (c) potential links to species in biological processes encompassing ternary interactions with vanadium and physiological targets.

Experimental Section

Materials and Methods. All experiments were carried out in the open air. Nanopure quality water was used for all reactions. VCl_3, V_2O_5, anhydrous citric acid, and H_2O_2 30% were purchased from Aldrich. Ammonia, ethanol, and 2-propanol were supplied by Fluka.

Physical Measurements. FT-IR measurements were taken on a Perkin-Elmer 1760X FT-IR spectrometer. UV−vis measurements were carried out on a Hitachi U2001 spectrophotometer in the range from 190 to 1000 nm. Elemental analyses were performed by Quantitative Technologies, Inc.

Solid State NMR. The high-resolution solid-state ^{13}C magic angle spinning (MAS) NMR spectra were measured at 75.47 MHz, on a Bruker MSL300 NMR spectrometer, capable of high power ^1H-decoupling. The spinning rate used for $^1H-^{13}C$ cross polarization and magic angle spinning experiments was 4.2 kHz at ambient

(5) (a) Djordjevic, C. In *Metal Ions in Biological Systems: Antitumorigenic Activity of Vanadium Compounds*; Sigel, H., Sigel, A., Eds.; Marcel Dekker: New York, 1995; Vol. 31, Chapter 18, pp 595−616. (b) Köpf-Maier, P.; Köpf, H. In *Metal Compounds in Cancer Therapy*; Fricker, S. P., Ed.; Chapman and Hall: London, 1994; pp 109−146. (c) Djordjevic, C.; Wampler, G. L. *J. Inorg. Biochem.* **1985**, *25*, 51−55.

(6) (a) Klarlund, J. K. *Cell* **1985**, *41*, 707−717. (b) Smith, J. B. *Proc. Natl. Acad. Sci. U.S.A.* **1983**, *80*, 6162−6167.

(7) (a) Walton, K. M.; Dixon, J. E. *Annu. Rev. Biochem.* **1993**, *62*, 101−120. (b) Lau, K.-H. W.; Farley, J. R.; Baylink, D. J. *Biochem. J.* **1989**, *257*, 23−36.

(8) (a) Brand, R. M.; Hamel, F. G. *Int. J. Pharm.* **1999,** *183*, 117−123. (b) Drake, P. G.; Posner, B. I. *Mol. Cell Biochem.* **1998**, *182*, 79−89. (c) Drake, P. G.; Bevan, A. P.; Burgess, J. W.; Bergeron, J. J.; Posner, B. I. *Endocrinology* **1996**, *137*, 4960−4968. (d) Eriksson, J. W.; Lönnroth, P.; Posner, B. I.; Shaver, A.; Wesslau, C.; Smith, U. P. *Diabetologia* **1996**, *39*, 235−242. (e) Stankiewicz, P. J.; Tracey, A. S. In *Metal Ions in Biological Systems: Stimulation of Enzyme Activity by Oxovanadium Complexes*; Sigel, H., Sigel, A., Eds.; Marcel Dekker: New York, 1995; Vol. 31, Chapter 8, pp 249−285.

(9) (a) Zimmet, P.; Alberti, K. G. M. M.; Shaw, J. *Nature* **2001**, *414*, 782−787. (b) Möller, D. E. *Nature* **2001**, *414*, 821−827. (c) Möller, D. E. *Nature* **2001**, *414*, 821−827.

(10) (a) Sakurai, H.; Kojima, Y.; Yoshikawa, Y.; Kawabe, K.; Yasui, H. *Coord. Chem. Rev.* **2002**, *226*, 187−198. (b) Sasagawa, T.; Yoshikawa, Y.; Kawabe, K.; Sakurai, H.; Kojima, Y. *J. Inorg. Biochem.* **2002**, *88*, 108−112. (c) Kanamori, K.; Nishida, K.; Miyata, N.; Okamoto, K.; Miyoshi, Y.; Tamura, A.; Sakurai, H. *J. Inorg. Biochem.* **2001**, *86*, 649−656. (d) Melchior, M.; Rettig, S. J.; Liboiron, B. D.; Thompson, K. H.; Yuen, V. G.; McNeill, J. H.; Orvig, C. *Inorg. Chem.* **2001**, *40*, 4686−4690. (e) Sun, Q.; Sekar, N.; Goldwaser, I.; Gershonov, E.; Fridkin, M.; Shechter, Y. *Am. J. Physiol.: Endocrinol. Metab.* **2000**, *279*, E403−E410. (f) Goldwaser, I.; Gefel, D.; Gershonov, E.; Fridkin, M.; Shechter, Y. *J. Inorg. Biochem.* **2000**, *80*, 21−25.

(11) (a) Crans, D. C. In *Metal Ions in Biological Systems: Vanadium and its Role in Life*; Sigel, H., Sigel, A., Eds.; Marcel Dekker: New York, 1995; Vol. 31, Chapter 5, pp 147−209. (b) Martin, R. B. *J. Inorg. Biochem.* **1986**, *28*, 181−187.

(12) (a) Kiss, T.; Buglyó, P.; Sanna, D.; Micera, G.; Decock, P.; Dewaele, D. *Inorg. Chim. Acta* **1995**, *239*, 145−153. (b) Crans, D. C.; Ehde, P. M.; Shin, P. K.; Pettersson, L. *J. Am. Chem. Soc.* **1991**, *113*, 3728−3736. (c) Crans, D. C.; Felty, R. A.; Miller, M. M. *J. Am. Chem. Soc.* **1991**, *113*, 265−269. (d) Tracey, A. S.; Li, H.; Gresser, M. J. *Inorg. Chem.* **1990**, *29*, 2267−2271. (e) Crans, D. C.; Bunch, R. L.; Theisen, L. A. *J. Am. Chem. Soc.* **1989**, *111*, 7597−7607.

(13) (a) Fritzsche, M.; Elvingson, K.; Rehder, D.; Pettersson, L. *Acta Chem. Scand.* **1997**, *51*, 483−491. (b) Ehde, P. M.; Andersson, I.; Pettersson, L. *Acta Chem. Scand.* **1991**, *45*, 998−1005. (c) Ehde, P. M.; Andersson, I.; Pettersson, L. *Acta Chem. Scand.* **1989**, *43*, 136−143. (d) Caldeira, M. M.; Ramos, M. L.; Oliveira, N. C.; Gil, S. V. M. *Can. J. Chem.* **1987**, *65*, 2434−2440.

(14) (a) Wright, D. W.; Humiston, P. A.; Orme-Johnson, W. H.; Davis, W. M. *Inorg. Chem.* **1995,** *34*, 4194−4197. (b) Zhou, Z.-H.; Wan, H.-L.; Tsai, K.-R. *Chin. Sci. Bull.* **1995**, *40*, 749. (c) Velayutham, M.; Varghese B.; Subramanian, S. *Inorg. Chem.* **1998**, *37*, 1336−1340. (d) Djordjevic, C.; Lee, M.; Sinn, E. *Inorg. Chem.* **1989**, *28*, 719−723.

(15) Tsaramyrsi, M.; Kaliva, M.; Giannadaki, T.; Raptopoulou, C. P.; Tangoulis, V.; Terzis, A.; Giapintzakis, J.; Salifoglou, A. *Inorg. Chem.* **2001**, *40*, 5772−5779.

(16) Tsaramyrsi, M.; Kavousanaki, D.; Raptopoulou, C. P.; Terzis, A.; Salifoglou, A. *Inorg. Chim. Acta* **2001**, *320*, 47−59.

temperature (25° C). The solid-state spectra resulted from the accumulation of 512 (**1**) and 1024 (**3**) scans. The recycle delay used was 4 s (**1**) and 2 s (**3**), the 90° pulse was 5 μs, and the contact time was 0.6 (**1** and **3**) ms. All solid-state spectra were referenced to methanol, which showed a peak at 45.17 ppm.

Solution NMR. The samples for solution NMR studies were prepared by dissolving the crystalline complexes **1** and **3** in D_2O. NMR spectra were recorded on a Bruker AM300 (^{13}C) spectrometer. Chemical shifts (δ) are reported in ppm relative to an internal reference of DSS.

Preparation of Complex $(NH_4)_6[V^V_2O_2(O_2)_2(C_6H_4O_7)_2]\cdot 4.5H_2O$ (1). Method 1. A sample of V_2O_5 (0.20 g, 1.1 mmol) was dissolved in 5 mL of H_2O, and a solution of ammonia (1:1 in water) was added slowly under stirring. The resulting slurry was heated and stirred overnight at 50 °C. On the following day, anhydrous citric acid (0.80 g, 4.2 mmol) was added under continuous stirring. Subsequently, the pH of the solution was adjusted with aqueous ammonia to 6.5, and the color turned orange-like. Stirring continued at room temperature for an additional 15 min. The reaction flask was subsequently placed on an ice bath, and hydrogen peroxide 30% (0.60 g, 18 mmol) was added slowly and under constant stirring. The solution turned yellow-orange and stayed as such. Then, the reaction flask was placed at 4 °C. On the following day, the color of the reaction had turned red with no further change. Cold ethanol was then added, and a few days later a red crystalline material precipitated out that was isolated by filtration and dried in vacuo. Yield: 0.23 g (28%). Anal. Calcd for **1**, $(NH_4)_6[V_2O_2(O_2)_2(C_6H_4O_7)_2]\cdot 4.5\ H_2O$ ($C_{12}H_{41}N_6O_{24.5}V_2$, MW = 763.39): C, 18.86; H, 5.37; N, 11.00. Found: C, 19.11; H, 5.75; N, 11.27.

Method 2. From VCl_3. An amount of VCl_3 (0.20 g, 1.3 mmol) was dissolved in 3 mL of water along with anhydrous citric acid (0.25 g, 1.3 mmol). The pH of the greenish reaction mixture was adjusted to 9.0 with aqueous ammonia (1:1 in water). The resulting reaction mixture was stirred overnight at room temperature. On the following day, the color turned blue and stayed as such. The reaction flask was, then, placed in an ice bath, and H_2O_2 30% (1.04 mL, 10.2 mmol) was added dropwise and under continuous stirring. The color of the solution turned orange-red, and stirring continued for up to 15 min without any further color change. Then, the reaction flask was placed at 4 °C. On the following day, the color of the reaction had turned red with no further change. Cold ethanol was then added, and a few days later red crystals formed that were isolated by filtration and dried in vacuo. Yield: 0.080 g (33%). Positive identification of the crystalline material as complex **1** came from the FT-IR spectrum and the X-ray unit cell determination carried out on a single crystal.

Thermal and pH-Dependent Interconversions. From $(NH_4)_6[V^V_2O_2(O_2)_2(C_6H_4O_7)_2]\cdot 4.5H_2O$ (1) to $(NH_4)_6[V^V_2O_4(C_6H_4O_7)_2]\cdot 6H_2O$ (2).[17] A quantity of complex $(NH_4)_6[V_2O_2(O_2)_2(C_6H_4O_7)_2]\cdot 4.5H_2O$ (0.15 g, 0.20 mmol) was placed in a 25 mL round-bottom flask and dissolved in 4 mL of water. The pH of the resulting red solution was ∼5.0. The solution was allowed to stir overnight at room temperature. On the following day, the color of the solution was light green, and the pH was ∼7.5. Subsequently, ethanol was added, and the reaction mixture was placed in the refrigerator. A few days later, yellowish crystals appeared at the bottom of the flask. The crystals were isolated by filtration and dried in vacuo. The yield was 0.050 g (33%). The FT-IR spectrum of the crystalline material was identical to that of an authentic sample of $(NH_4)_6[V^V_2O_4(C_6H_4O_7)_2]\cdot 6H_2O$.[17] Further proof on the identity of the crystalline product was provided by the X-ray unit cell determination of one of the isolated single crystals.

From $(NH_4)_6[V^V_2O_4(C_6H_4O_7)_2]\cdot 6H_2O$ (2) to $(NH_4)_6[V^V_2O_2(O_2)_2(C_6H_4O_7)_2]\cdot 4.5H_2O$ (1). A quantity of complex $(NH_4)_6[V^V_2O_4(C_6H_4O_7)_2]\cdot 6H_2O$ (0.57 g, 0.75 mmol) was placed in a 25 mL round-bottom flask and dissolved in 3 mL of water. The pH of the resulting yellowish solution was ∼6.5. The solution was placed in an ice bath, and a hydrogen peroxide solution 30% (0.40 g, 12 mmol) was added slowly and under continuous stirring. Subsequently, the new reaction mixture was allowed to stir on ice for an additional 10 min. During that period of time, the color of the solution turned orange and stayed as such. Then, the reaction flask was placed at 4 °C. On the following day, the color of the reaction had turned red with no further change. Cold ethanol was then added, and a few days later, red crystals appeared at the bottom of the flask. The crystals were isolated by filtration and dried in vacuo. The yield was 0.30 g (53%). The FT-IR of the crystalline material was identical to that of an authentic sample of $(NH_4)_6[V^V_2O_2(O_2)_2(C_6H_4O_7)_2]\cdot 4.5H_2O$. Further proof on the identity of the crystalline product was provided by the X-ray unit cell determination of one of the isolated single crystals.

From $(NH_4)_6[V^V_2O_2(O_2)_2(C_6H_4O_7)_2]\cdot 4.5H_2O$ (1) to $(NH_4)_4[V^{IV}_2O_2(C_6H_4O_7)_2]\cdot 2H_2O$[15] (4). A quantity of $(NH_4)_6[V^V_2O_2(O_2)_2(C_6H_4O_7)_2]\cdot 4.5H_2O$ (0.12 g, 0.16 mmol) was dissolved in 4 mL of water, in a 25 mL round-bottom flask. The pH of the resulting solution was ∼5.0. The solution was allowed to stir overnight at 50 °C. On the following day, the color of the solution was blue, and the pH was ∼7.0. No further changes were observed upon prolonged stirring and heating of the solution. Subsequently, the solution was evaporated to dryness by means of a rotary evaporator. The residue was then redissolved in a minimum amount of a water/2-propanol mixture (1:1 v/v), and the resulting blue solution was placed in the refrigerator (4 °C). A week or so later, blue crystals appeared at the bottom and on the sides of the flask. They were isolated by filtration and dried in vacuo. The yield of the transformation was 0.035 g (36%). The FT-IR spectrum of the crystalline material in corroboration with the X-ray unit cell determination of one of the isolated single crystals revealed that the product of the transformation was $(NH_4)_4[V^{IV}_2O_2(C_6H_4O_7)_2]\cdot 2H_2O$.[15]

From $(NH_4)_6[V^V_2O_2(O_2)_2(C_6H_4O_7)_2]\cdot 4.5H_2O$ (1) to $(NH_4)_2[V^V_2O_2(O_2)_2(C_6H_6O_7)_2]\cdot 2H_2O$[16] (3). A quantity of $(NH_4)_6[V^V_2O_2(O_2)_2(C_6H_4O_7)_2]\cdot 4.5H_2O$ (0.14 g, 0.19 mmol) was dissolved in 4 mL of water, in a 25 mL round-bottom flask on ice. The pH of the resulting solution was ∼5.0. Using a cold solution of dilute hydrochloric acid, the pH of the solution was adjusted to ∼3.5. As a result of this adjustment, the color of the solution turned dark red and stayed as such. No further changes were observed upon stirring of the solution on ice for up to 15 min. Subsequently, the solution was placed in the refrigerator (4 °C). Addition of cold ethanol afforded a week or so later red crystals at the bottom and on the sides of the flask. They were isolated by filtration and dried in vacuo. The yield of the transformation was 0.040 g (34%). The FT-IR spectrum of the crystalline material and the X-ray unit cell determination of one of the isolated single crystals revealed that the product of the transformation was $(NH_4)_2[V^V_2O_2(O_2)_2(C_6H_6O_7)_2]\cdot 2H_2O$.[16]

X-ray Crystallography. Crystal Structure Determination. X-ray quality crystals of compound **1** were grown from water−ethanol mixtures. A single crystal, with dimensions 0.06 × 0.16 × 0.36 mm^3 (**1**), was mounted on a Crystal Logic dual-goniometer diffractometer, using graphite monochromated Mo Kα radiation. Unit cell dimensions for **1** were determined and refined by using

(17) Kaliva, M.; Raptopoulou, C. P.; Terzis, A.; Salifoglou, A. *J. Inorg. Biochem.* **2003**, *93*, 161−173.

Table 1. Summary of Crystal, Intensity Collection, and Refinement Data for $(NH_4)_6[V_2O_2(O_2)_2(C_6H_4O_7)_2]\cdot 4.5H_2O$ (**1**)

formula	$C_{12}H_{41}N_6O_{24.5}V_2$
fw	763.39
temp, K	298
wavelength	Mo Kα 0.71073
space group	*C*2/*c*
a (Å)	12.391(5)
b (Å)	15.737(7)
c (Å)	17.102(7)
β, deg	110.84(1)
V, (Å^3)	3117(1)
Z	4
D_{calcd}/D_{measd} (Mg m^{-3})	1.627/1.63
abs coeff (μ), mm^{-1}	0.703
range of *h*, *k*, *l*	$-14 \rightarrow 13$ $-18 \rightarrow 0$ $0 \rightarrow 20$
GOF on F^2	1.051
w^a	$a = 0.0970$, $b = 8.0385$
R^b	$R = 0.0519^c$
$R_w{}^b$	$R_w = 0.1475^c$

[a] $w = 1/[\sigma^2(F_o^2) + (aP)^2 + bP]$ where $P = (\max(F_o^2, 0) + 2F_c^2)/3$ [b] R values are based on F values, R_w values are based on F^2. $R = (\sum||F_o| - |F_c||)/(\sum(|F_o|))$, $R_w = \sqrt{\sum[w(F_o^2-F_c^2)^2]/\sum[w(F_o^2)^2]}$. [c] For 2223 reflections with $I > 2\sigma(I)$.

the angular settings of 25 automatically centered reflections in the range $11° < 2\theta < 23°$. Relevant crystallographic details are given in Table 1. Intensity data were measured by using $\theta-2\theta$ scans. Three standard reflections were monitored every 97 reflections, throughout data collection, and showed less than 3% variation and no decay. Lorentz, polarization, and ψ-scan absorption corrections were applied by using Crystal Logic software. Further experimental crystallographic details for **1**: $2\theta_{max} = 50$ °; scan speed 1.8°/min; scan range $2.3 + \alpha_1\alpha_2$ separation; reflections collected/unique/used, 2829/2733 ($R_{int} = 0.0291$)/2723; 261 parameters refined; $(\Delta/\sigma)_{max} = 0.003$; $(\Delta\rho)_{max}/(\Delta\rho)_{min} = 0.726/-0.453$ e/Å^3; GOF on $F^2 = 1.051$; R/R_w (for all data), 0.0644/0.1623.

The structure of complex **1** was solved by direct methods using SHELXS-86,[18] and refined by full-matrix least-squares techniques on F^2 with SHELXL-93.[19] All non-H atoms in the structure of **1** were refined anisotropically. All the H-atoms in **1** were located by difference maps and were refined isotropically.

Results

Syntheses. The complex $(NH_4)_6[V^V_2O_2(O_2)_2(C_6H_4O_7)_2]\cdot 4.5\ H_2O$ (**1**) was synthesized from simple reagents in aqueous solutions. In a typical reaction, V_2O_5 reacted with citric acid in the presence of ammonia at pH ~6.5. Aqueous ammonia was important for two reasons. It helped adjust the pH of the reaction medium at which the specific synthesis was carried out, and at the same time provided the cations necessary for balancing the negative charge on the derived anionic complex **1**. The overall stoichiometric reaction (Reaction **1**) leading to complex **1** is shown schematically:

$$V_2O_5 + 2C_6H_8O_7 + 6OH^- + 2H_2O_2 \rightarrow [V_2O_2(O_2)_2(C_6H_4O_7)_2]^{6-} + 9H_2O \quad (1)$$

A redox reaction for the synthesis of **1** was also employed, with VCl_3 and citric acid reacting in the presence of hydrogen peroxide. The reaction (Reaction 2) was similar to that used for the synthesis of $(NH_4)_6[V^V_2O_4(C_6H_4O_7)_2]\cdot 6H_2O$ (**2**).[17] Initially, VCl_3 and citric acid reacted in water at pH ~ 9, in the presence of ammonia, to provide a blue solution. Hydrogen peroxide was then added to that reaction mixture, ultimately affording a red crystalline material, the composition of which was consistent with **1** (vide infra).

$$2VCl_3 + 2C_6H_8O_7 + {}^1/_2O_2 + 12OH^- + 3H_2O_2 \xrightarrow{pH \sim 9} [V_2O_2(O_2)_2(C_6H_4O_7)_2]^{6-} + 6Cl^- + 13H_2O \quad (2)$$

Previous results on the relevant chemistry had shown that the blue species arising in the course of the reaction was a dinuclear vanadium(IV)−citrate species, for which the properties and structure had been determined.[15]

Of the two different routes employed for the synthesis of complex **1**, one involved oxidation of vanadium(III) to vanadium(V). In both cases, precipitation of the products from the reaction mixture, in a crystalline form, was achieved by addition of ethanol at 4 °C. Elemental analysis on the NH_4^+ salt of the isolated crystalline materials suggested the formulation $(NH_4)_6[V^V_2O_2(O_2)_2(C_6H_4O_7)_2]\cdot 4.5H_2O$. Positive identification of the crystalline products was achieved by FT-IR spectroscopy and determination of the crystal cell unit constants by X-ray crystallography for one of the isolated single crystals from **1**. Complex **1** is stable, in the crystalline form, in the air, for long periods of time. It is insoluble in alcohols (CH_3OH, i-PrOH), acetonitrile, and dimethyl sulfoxide (DMSO) at room temperature. It readily dissolves in water.

Interconversions. In view of the acid−base reactivity previously observed between pairs of the non-peroxo dinuclear complexes $[V^V_2O_4(C_6H_4O_7)_2]^{6-}$ and $[V^V_2O_4(C_6H_6O_7)_2]^{2-}$, which had been synthesized, isolated, and characterized crystallographically,[16,17,20] an analogous behavior was thought to exist between peroxo-containing dinuclear vanadium complexes (Figure 1). To this end, a pH-dependent transformation was carried out between complexes $(NH_4)_6[V^V_2O_2(O_2)_2(C_6H_4O_7)_2]\cdot 4.5\ H_2O$ (**1**) and $(NH_4)_2[V^V_2O_2(O_2)_2(C_6H_6O_7)_2]\cdot 2\ H_2O$ (**3**). Specifically, simple dissolution of complex **1** in water and adjustment of pH to a final value of ~3.5, with aqueous hydrochloric acid, led to the isolation of complex $(NH_4)_2[V^V_2O_2(O_2)_2(C_6H_6O_7)_2]\cdot 2H_2O$ (**3**) upon addition of ethanol at 4 °C. The stoichiometric reaction (Reaction 3) taking place is shown here:

$$[V_2O_2(O_2)_2(C_6H_4O_7)_2]^{6-}\ (\mathbf{1}) + 4H^+ \rightarrow [V_2O_2(O_2)_2(C_6H_6O_7)_2]^{2-} \quad (3)$$

This pH-dependent transformation led to a crystalline product, which was positively identified by its well-known FT-IR signature and through unit cell constant determination

(18) Sheldrick, G. M. *SHELXS-86: Structure Solving Program*; University of Göttingen: Göttingen, Germany, 1986.
(19) Sheldrick, G. M. *SHELXL-93: Structure Refinement Program*; University of Göttingen: Göttingen, Germany, 1993.
(20) Zhou, Z.-H.; Yan, W.-B.; Wan, H.-L.; Tsai, K.-R.; Wang, J.-Z.; Hu, S.-Z.; *Chem. Crystallogr.* **1995**, *25*, 807−811.

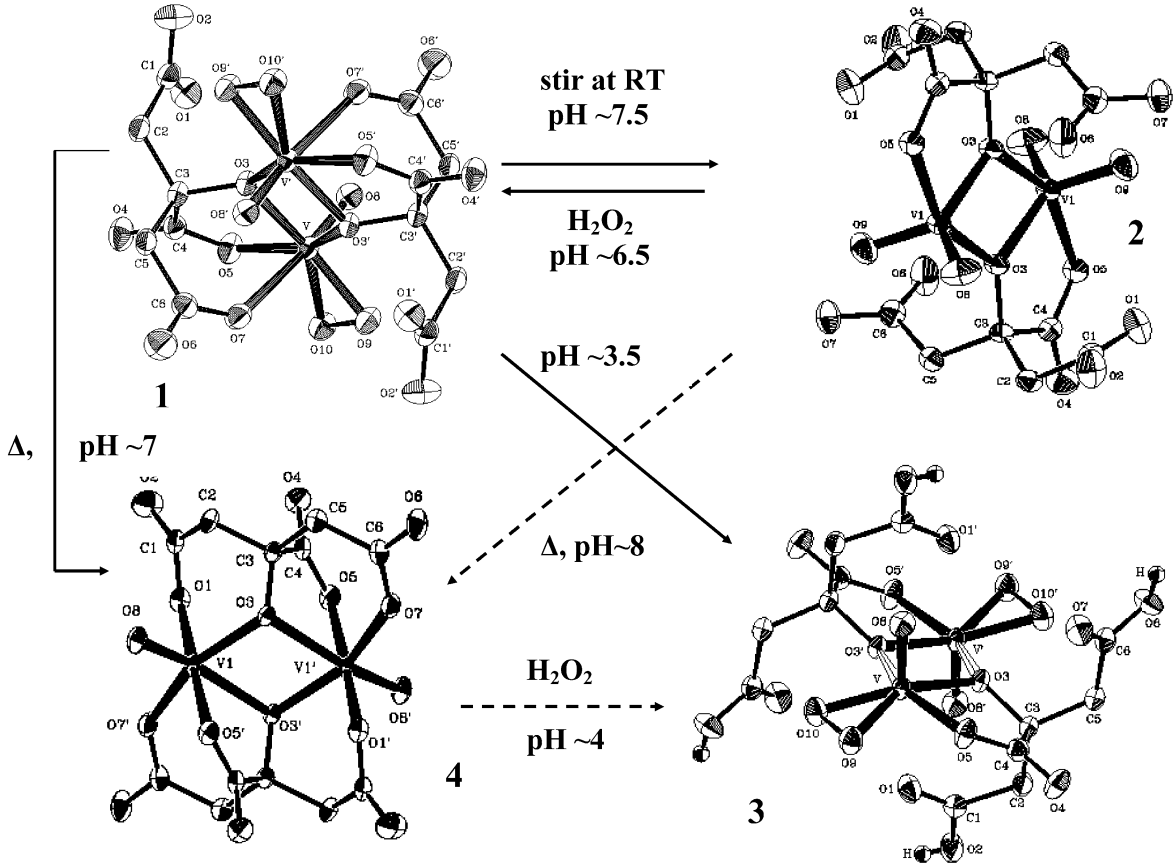

Figure 1. Scheme of pH-dependent and thermal transformations among various vanadium(IV,V)−citrate anionic complexes. Dashed arrows reflect previously established interconversions between vanadium−citrate species.

by X-ray crystallography. Beyond the significance of pH-dependent connectivity between the two species, it appears that, from the synthetic point of view, the aforementioned transformation could serve as an additional method for the synthesis and isolation of complex **3** from the well-known dinuclear species $(NH_4)_6[V^V_2O_2(O_2)_2(C_6H_4O_7)_2]\cdot 4.5\ H_2O$ (**1**) and vice versa.

In a thermally induced transformation, solutions of complex **1** lost their reddish color and converted to a blue solution, which retained its coloration even after returning the reaction vessel to room temperature. Addition of 2-propanol resulted in the isolation of the well-known and characterized vanadium(IV)-containing dinuclear species $(NH_4)_4[V^{IV}_2O_2(C_6H_4O_7)_2]\cdot 2H_2O$ (**4**).[15] Under the optimally employed experimental conditions of this transformation, no other species could be isolated. It should be noted that the starting material is a complex containing vanadium(V), in contrast to the derived product, complex **4**, which contains vanadium(IV). Therefore, what essentially occurs here is a redox reaction leading to the reduction of the vanadium(V) species (vide supra).

To further inquire into mechanistic aspects of this transformation, a solution of **1** was allowed to stir overnight at room temperature. A day later, the color of the originally reddish compound **1** had turned oily yellow and stayed as such. Addition of ethanol afforded a few days later a crystalline material, which was identified as complex **2** by FT-IR spectroscopy and X-ray crystallography. A plausible rendition of the process is shown here:

$$[V_2O_2(O_2)_2(C_6H_4O_7)_2]^{6-}\ (\mathbf{1}) + 2H_2O \xrightarrow{\text{stir at RT}} [V_2O_4(C_6H_4O_7)_2]^{6-}\ (\mathbf{2}) + 2H_2O_2$$

It appears, therefore, that in this transformation of complex **1**, the peroxide group O_2^{2-} departs early on from the complex assembly resulting in complex **2**. Complex **2**, subsequently, under the influence of heat is transformed into complex **4**, containing vanadium(IV).

The reverse process of peroxide addition onto complex **2** was also investigated leading to the fully peroxidized complex **1**. Thus, a reversible interconversion between **1** and **2** was delineated, linking the two species directly or indirectly with the vanadium(IV) complex **4**. The stoichiometric reaction depicting the conversion of **2** to **1** is shown here:

$$[V_2O_4(C_6H_4O_7)_2]^{6-}\ (\mathbf{2}) + 2H_2O_2 \xrightarrow{\text{stir in ice bath}} [V_2O_2(O_2)_2(C_6H_4O_7)_2]^{6-}\ (\mathbf{1}) + 2H_2O$$

X-ray Crystallographic Structure. $(NH_4)_6[V^V_2O_2(O_2)_2(C_6H_4O_7)_2]\cdot 4.5H_2O$ (1). The X-ray crystal structure of **1** consists of discrete anions and ammonium cations. Complex **1** crystallizes in the monoclinic system *C*2/*c* with four molecules in the unit cell. The ORTEP diagram of the anion in **1** is shown in Figure 1. A select list of interatomic

Table 2. Bond Lengths [Å] and Angles [deg] for **1**[a]

V−O(8)	1.597(3)	O(8)−V−O(10)	99.91(13)
V−O(10)	1.894(3)	O(8)−V−O(9)	101.44(13)
V−O(9)	1.895(3)	O(10)−V−O(9)	44.34(12)
V−O(3)	2.013(3)	O(8)−V−O(3)	98.06(12)
V−O(5)	2.022(3)	O(10)−V−O(3)	150.26(11)
V−O(3)′	2.055(3)	O(9)−V−O(3)	151.19(11)
V−O(7)	2.322(3)	O(8)−V−O(5)	93.68(13)
O(3)−C(3)	1.431(4)	O(10)−V−O(5)	77.40(12)
O(3)−V′	2.055(3)	O(9)−V−O(5)	121.31(12)
O(5)−C(4)	1.282(5)	O(3)−V−O(5)	77.96(11)
O(7)−C(6)	1.260(5)	O(8)−V−O(3)′	97.78(12)
O(9)−O(10)	1.430(4)	O(10)−V−O(3)′	126.73(11)
C(1)−O(2)	1.262(5)	O(9)−V−O(3)′	83.01(11)
C(1)−O(1)	1.263(5)	O(3)−V−O(3)′	73.44(11)
C(1)−C(2)	1.509(5)	O(5)−V−O(3)′	150.37(10)
C(2)−C(3)	1.535(5)	O(8)−V−O(7)	173.66(12)
C(3)−C(5)	1.526(5)	O(10)−V−O(7)	83.05(11)
C(3)−C(4)	1.540(5)	O(9)−V−O(7)	84.62(11)
C(4)−O(4)	1.228(5)	O(3)−V−O(7)	77.03(10)
C(5)−C(6)	1.524(5)	O(5)−V−O(7)	81.44(11)
C(6)−O(6)	1.257(5)	O(3)′−V−O(7)	84.74(11)
		C(3)−O(3)−V	114.0(2)
		C(3)−O(3)−V′	127.6(2)
		V−O(3)−V′	106.56(11)
		C(4)−O(5)−V	117.3(2)
		C(6)−O(7)−V	132.5(2)
		O(10)−O(9)−V	67.8(2)
		O(9)−O(10)−V	67.8(2)
		O(2)−C(1)−O(1)	122.9(4)
		O(2)−C(1)−C(2)	119.5(4)
		O(1)−C(1)−C(2)	117.6(3)
		C(1)−C(2)−C(3)	114.5(3)
		O(3)−C(3)−C(5)	111.5(3)
		O(3)−C(3)−C(2)	111.0(3)
		C(5)−C(3)−C(2)	109.7(3)
		O(3)−C(3)−C(4)	107.3(3)
		C(5)−C(3)−C(4)	107.6(3)
		C(2)−C(3)−C(4)	109.6(3)
		O(4)−C(4)−O(5)	124.1(3)
		O(4)−C(4)−C(3)	120.4(3)
		O(5)−C(4)−C(3)	115.3(3)
		C(6)−C(5)−C(3)	115.1(3)
		O(6)−C(6)−O(7)	123.6(4)
		O(6)−C(6)−C(5)	116.1(3)
		O(7)−C(6)−C(5)	120.2(3)

[a] Symmetry transformations used to generate equivalent atoms: ′ $-x$, $-y+1$, $-z$.

distances and bond angles for **1** is provided in Table 2. The anionic complex in **1** consists of a $V^V_2O_2$ core with the two vanadium ions in the oxidation state +5. The rhombic core unit is planar, due to the presence of a center of inversion. The two oxygen bridges derive from the alkoxide moieties of the two citrate ligands attached to the core. Each vanadium ion is bound to a doubly bonded oxygen, with the remaining sites being occupied by oxygens from the citrate ligands and a peroxo group O_2^{2-}. The citrates participating in the coordination sphere around each vanadium ion are quadruply deprotonated. As such, they coordinate through the central alkoxide and carboxylate as well as one of the terminal carboxylate groups. The remaining terminal carboxylate group, albeit deprotonated, is not bound to the vanadium ions. The coordination environment around each vanadium ion is pentagonal bipyramidal, with the peroxo group, the two bridging alkoxide oxygens, and the central carboxylate oxygen lying in the equatorial plane, and the doubly bonded oxygen of the $V^V_2O_2$ core and the terminal carboxylate oxygen occupying the apical position.

The V−O bond distances in **1** are similar to the corresponding distances in other vanadium(V)−peroxo−citrate dimers such as $(NH_4)_2[V_2O_2(O_2)_2(C_6H_6O_7)_2]\cdot 2H_2O$ (1.873(2)−2.034(2) Å) (**3**),[16] $K_2[V_2O_2(O_2)_2(C_6H_6O_7)_2]\cdot 2H_2O$ (1.873(1)−2.039(1) Å) (**5**),[14d] $(NH_4)_4[V_2O_2(O_2)_2(C_4H_3O_5)_2]\cdot 3H_2O$ (1.859(3)−2.294(3) Å) (**6**),[21] $K_4[V_2O_2(O_2)_2(C_4H_3O_5)_2]\cdot 4H_2O$ (1.868(2)−2.248(2) Å) (**7**),[21] $K_2[V_2O_2(O_2)_2(C_4H_4O_5)_2]\cdot 2H_2O$ (1.869(2)−2.033(2) Å) (**8**),[21] and non-peroxo congener species such as $(NH_4)_6[V_2O_4(C_6H_4O_7)_2]\cdot 6H_2O$ (1.966(2)−2.017(2) Å) (**9**),[17] $K_4[V_2O_4(C_6H_5O_7)_2]\cdot 5.6H_2O$ (1.966(2)−2.017(2) Å),[22] $Cs_2[V_2O_4(C_4H_4O_5)_2]\cdot 2H_2O$ (1.963(4)−2.016(4) Å),[23] $(NH_4)_2[V(O)_2(OC(CH_2CH_3)_2COO)]_2$ (1.973(1)−1.984(2) Å),[24] and $Na_2[V_2O_4(C_4H_6O_3)_2]\cdot 7H_2O$ (1.990(1)−2.004(1) Å).[25] The V═O bond distance is similar to those in the congener complexes **5**−**8** (1.585(2)−1.606(2) Å). The angles in complex **1** are similar to those observed in a number of $V^V_2O_2$ core-containing dimers, exhibiting pentagonal bipyramidal geometry around the vanadium(V) ions.[21] It should be emphasized that the two uncoordinated terminal carboxylate groups in **1** do not differ in their protonation state. They both abstain from binding to the $V^V_2O_2$ core like the corresponding groups in **5** and **8** (low-pH analogues), which are, however, protonated.

The citrate ligands in the anion of **1** adopt an extended conformation upon binding to the vanadium ion. The carbon atoms C(1), C(2), C(3), C(5), and C(6) of the citrate backbone are coplanar, with the largest standard deviation being 0.08 Å for C(6). The central carboxylate plane O(4)−C(4)−O(5) is rotated ∼11.7° out of the O(3)−C(3)−C(4) plane. These values are in line with those seen in other vanadium(V)−peroxo−carboxylate complexes, suggesting a similar approach of the citrate to the metal ion in all cases of complex assemblies.

The V····V distance in the anion of **1** is 3.261(1) Å. This value is similar to those observed in vanadium(V)−peroxo−carboxylate dinuclear complexes reported in the past ((**3**) 3.245(2) Å,[16] (**5**) 3.262(1) Å,[14d] (**7**) 3.254(1) Å).[21]

Six ammonium counterions are present in **1**. They counterbalance the 6− charge generated on the complex anion. The cations are in contact with the carboxylate oxygens of the citrate anion and the lattice water oxygens. The presence of water molecules of crystallization in **1** contribute to the formation of an extensive hydrogen-bonding network (Table 3).

UV−Vis Spectroscopy. The electronic spectrum of **1** was taken in H_2O. The spectrum showed a band at 410 nm (ϵ = 327 M^{-1} cm^{-1}) with a rising absorbance into the ultraviolet region. An additional feature appeared at around 203 nm (ϵ = 6941 M^{-1} cm^{-1}). The spectrum was featureless beyond 420 nm. The band at 410 nm has been attributed to the

(21) Kaliva, M.; Giannadaki, T.; Raptopoulou, C. P.; Tangoulis, V.; Terzis, A.; Salifoglou, A. *Inorg. Chem.* **2001**, *40*, 3711−3718.
(22) Kaliva, M.; Giannadaki, T.; Raptopoulou, C. P.; Terzis, A.; Salifoglou, A. *Inorg. Chem.* **2002**, *41*, 3850−3858.
(23) Biagioli, M.; Strinna-Erre, L.; Micera, G.; Panzanelli, A.; Zema, M. *Inorg. Chim. Acta* **2000**, *310*, 1−9.
(24) Hambley, T. W.; Judd, R. J.; Lay, P. A. *Inorg. Chem.* **1992**, *31*, 345−351.
(25) Bourne, S. A.; Cruywagen, J. J.; Kleinhorst, A. *Acta Crystallogr.* **1999**, *C55*, 2002−2004.

Table 3. Hydrogen Bonds in $(NH_4)_6[V_2O_2(O_2)_2(C_6H_4O_7)_2]\cdot 4.5H_2O$

interaction	D···A (Å)	H···A (Å)	D−H···A (deg)	symmetry operation
N1−HN1A···O7	2.793	1.899	170.4	$0.5 - x, 0.5 - y, -z$
N1−HN1B···O2	2.959	2.106	164.3	$0.5 + x, -0.5 + y, z$
N1−HN1C···O2	2.852	2.029	174.9	$-x, 1 - y, -z$
N1−HN1D···OW2	3.167	2.194	173.2	$0.5 - x, -0.5 + y, 0.5 - z$
N2−HN2A···O6	2.887	1.864	178.1	$0.5 - x, 1.5 - y, -z$
N2−HN2B···O10	2.977	2.200	178.0	$0.5 - x, 0.5 + y, 0.5 - z$
N2−HN2C···OW2	2.953	1.951	156.3	x, y, z
N2−HN2D···O1	2.877	2.034	169.2	x, y, z
N3−HN3A···O1	2.855	2.021	167.8	x, y, z
N3−HN3B···O6	3.096	2.229	164.1	$x, 1 - y, 0.5 + z$
N4−HN4A···OW1	2.936	2.174	170.6	$0.5 - x, 0.5 + y, 0.5 - z$
N4−HN4B···O2	2.906	2.159	160.3	$-x, y, 0.5 - z$
OW1−HW1A···O6	2.779	1.563	160.7	$x, 1 - y, 0.5 + z$
OW1−HW1B···O5	2.695	1.660	144.4	x, y, z
OW2−HW2A···O4	2.840	1.839	171.7	$1 - x, y, 0.5 - z$
OW2−HW2B···OW1	2.850	1.770	157.0	x, y, z

presence of a peroxo to vanadium ligand to metal charge transfer (LMCT).[26] It appears, therefore, that, at the pH examined here, the peroxo group remains attached to the vanadium ion, as that is indicated by a similar LMCT absorption at 340 nm in complex **6**,[21] further supporting the idea of a stable $[(V{=}O)(O_2)]^+$ unit in both classes of complexes. The presence of the weak LMCT band, as surmised by Evans,[27] was also observed in other vanadium−peroxo−citrate complexes bearing a $[(V{=}O)_2O_2(O_2)_2]^0$ core,[14d,16,21] and was reasonably assigned to a $\pi_v^* \rightarrow$ d transition.[26,27] The intense absorption band at 203 nm in **1**, in the ultraviolet region, may be associated with the $\pi_h^* \rightarrow$ dσ^* LMCT transition. This transition had been previously proposed to occur at even higher energies than the $\pi_v^* \rightarrow$ d transition, due to the stabilization of the π_h^* σ peroxo to metal bonding orbital. Further definitive assignments cannot be made, presently, due to the lack of in-depth spectroscopic studies.[26,27] The intensity of the LMCT band at 410 nm stays constant for a short period of time, beyond which it dwindles progressively (vide infra), thus signifying the long-term instability of aqueous solutions of **1**.

FT-IR Spectroscopy. The FT-IR spectrum of **1** was recorded in KBr and reveals the presence of vibrationally active carboxylate groups. Antisymmetric and symmetric vibrations for the carboxylate groups of the coordinated citrate ligands were present. In particular, antisymmetric stretching vibrations $\nu_{as}(COO^-)$ were present for the carboxylate carbonyls in the range 1631−1569 cm^{-1}. Symmetric vibrations $\nu_s(COO^-)$ for the same groups were present around 1399 cm^{-1}. The observed carbonyl vibrations were shifted to lower frequency values in comparison to the corresponding vibrations in free citric acid, suggesting changes in the vibrational status of the citrate ligand coordinated to the vanadium.[28] The difference between the symmetric and antisymmetric stretches, $\Delta(\nu_{as}(COO^-) - \nu_s(COO^-))$, was greater than 200 cm^{-1}, indicating that the citrate carboxylate groups were either free or coordinated to vanadium in a monodentate fashion.[28] The latter contention was confirmed by the X-ray crystal structure of **1**. Furthermore, the $\nu(V{=}O)$ vibrations for the $VO(O_2)^+$ groups in **1** were present in the range 965−952 cm^{-1}. The peroxo $\nu(O{-}O)$ stretch was attributed to vibrations at 930 cm^{-1}. The described tentative assignments were in agreement with previous reports on dinuclear V(V)−peroxo complexes,[14d,16,21] and consistent with infrared frequencies attributed to carboxylate-containing ligands bound to different metal ions.[29−31]

Solid State NMR Spectroscopy. The MAS ^{13}C NMR spectrum of **1** showed discrete resonances for the various citrate carbons. Specifically, two of the resonances lie in the high field region whereas three other resonances appear in the low field region. The signals in the high field region could be assigned to the methylene carbons (40.0 and 44.8 ppm) located adjacent to the two terminal carboxylates of the citrate ligand. The resonance at 86.8 ppm is reasonably attributed to the central carbon atom located adjacent to the bound central carboxylate group. In the low field region, where the carbonyl carbon resonances are expected, there were two signals observed (173.5 and 177.1 ppm) for the terminal carboxylate groups, one bound to one of the two V(V) ions of the central core with the second one abstaining from coordination. There was also one signal observed (186.8 ppm) for the bound central carboxylate carbon of the citrate ligand. This signal is shifted to lower field by 13.3 and 9.7 ppm in comparison to the previous two signals for the terminal carboxylate groups, most likely due to the presence of the nearby ionized alkoxide group. The solid state NMR spectrum was also taken for **3**. There, the high field resonances in the region from 43 to 48 ppm were assigned to the methylene carbons abutting the two uncoordinated terminal carboxylates of the citrate ligand. The resonance at 87.6 ppm was reasonably assigned to the central carbon of the citrate ligand, whereas the signals at 179.7 and 181.6 ppm, and 182.1 ppm, were attributed to the terminal and central carboxylate carbons, respectively. A similar pattern of ^{13}C resonances was observed in the case of mononuclear complexes, such as $(NH_4)_5[Al(C_6H_4O_7)_2]\cdot 2H_2O$,[31e] the dinuclear complex $(NH_4)_4[Ti_2(O_2)_2(C_6H_4O_7)_2]\cdot 2H_2O$,[32] and dinuclear complexes such as $Na_2[Bi_2(C_6H_4O_7)_2]\cdot 7H_2O$.[33] In the latter case, fully resolved resonances were observed for

(26) Lever, A. B. P.; Gray, H. B. *Inorg. Chem.* **1980**, *19*, 1823−1824. (b) Lever, A. B. P.; Gray, H. B. *Acc. Chem. Res.* **1978**, *11*, 348−355.
(27) Evans, D. F. *J. Chem. Soc.* **1957**, 4013−4018.
(28) Deacon, G. B.; Philips, R. *J. Coord. Chem. Rev.* **1980**, *33*, 227−250.
(29) Griffith, W. P.; Wickins, T. D. *J. Chem. Soc. A* **1968**, 397−400.
(30) Vuletic, N.; Djordjevic, C. *J. Chem. Soc., Dalton Trans.* **1973**, 1137−1141.
(31) (a) Matzapetakis, M.; Raptopoulou, C. P.; Terzis, A.; Lakatos, A.; Kiss, T.; Salifoglou, A. *Inorg. Chem.* **1999**, *38*, 618−619. (b) Matzapetakis, M.; Raptopoulou, C. P.; Tsohos, A.; Papefthymiou, B.; Moon, N.; Salifoglou, A. *J. Am. Chem. Soc.* **1998**, *120*, 13266−13267. (c) Matzapetakis, M.; Dakanali, M.; Raptopoulou, C. P.; Tangoulis, V.; Terzis, A.; Moon, N.; Giapintzakis, J.; Salifoglou, A. *J. Biol. Inorg. Chem.* **2000**, *5*, 469−474. (d) Matzapetakis, M.; Karligiano, N.; Bino, A.; Dakanali, M.; Raptopoulou, C. P.; Tangoulis, V.; Terzis, Giapintzakis, J.; Salifoglou, A. *Inorg. Chem.* **2000**, *39*, 4044−4051. (e) Matzapetakis, M.; Kourgiantakis, M.; Dakanali, M.; Raptopoulou, C. P.; Terzis, A.; Lakatos, A.; Kiss, T.; Banyai, I.; Iordanidis, L.; Mavromoustakos, T.; Salifoglou, A. *Inorg. Chem.* **2001**, *40*, 1734−1744.
(32) Dakanali, M.; Kefalas, E. T.; Raptopoulou, C. P.; Terzis, A.; Voyiatzis, G.; Kyrikou, I.; Mavromoustakos, T.; Salifoglou, A. *Inorg. Chem.* **2003**, *42*, 4632−4639.
(33) Barrie, P. J.; Djuran, M. I.; Mazid, M A.; McPartlin, M.; Sadler, P. J.; Scowen, I. J.; Sun, H. *J. Chem. Soc., Dalton Trans.* **1996**, 2417−2422.

the carbons of the two variably bound CH_2COO^- groups (one is bound in a bidentate fashion to the bismuth ion, whereas the other one serves as a bridge to two bismuth ions).

Solution NMR Spectroscopy. The solution ^{13}C NMR spectra of complexes **1** and **3** were also measured in D_2O. The spectra revealed the presence of several resonances. There were two resonances in the high field region (45.0 and 47.9 ppm (**1**) and 40.7 and ~45.7 ppm (**3**)), which were attributed to the CH_2 groups of the citrate ligands bound to the V(V) ion. The resonance at 85.1 ppm (**1**) and 85.9 ppm (**3**) was assigned to the central carbon of the bound citrate. The signals at 179.5 and 180.1 ppm (**1**) and ~175.2 ppm (**3**) in the lower field region were assigned to the terminal carboxylate carbons. The resonance located at low field (180.8 ppm (**1**) and 178.0 ppm (**3**)) was attributed to the central carboxylate carbon. This signal was shifted to lower fields in comparison to the other signal(s) belonging to the terminal carboxylate carbons. In this case as well, the shift was most likely due to the presence of the central carboxylate carbon close to the deprotonated alkoxide group. It is worth noting that the patterns of resonances observed in both **1** and **3** were similar to those in the corresponding solid state MAS ^{13}C NMR spectra. Due to the length of time required for collection of ^{13}C NMR data, decomposition of **1** and **3** was also observed (free citrate, non-peroxo species, etc.), in consonance with the limited stability of those complexes in solution, thus hampering the detailed identification of all species in the spectra (more so in the case of **3**). That, however, does not detract or diminish the significance of the observed resonance patterns of interest, and the consistency between the solid and solution state spectra, which collectively support the distinct nature of complexes **1** and **3**.

Discussion

The Aqueous Vanadium(V)−Peroxo−Citrate Chemistry. The synthetic aqueous vanadium(V)−peroxo−citrate chemistry has provided a new species, complex **1**, in a series of related dinuclear complexes exhibiting various structural similarities and differences among them. The newly arisen species confirmed the diversity in the chemical reactivity of peroxo−vanadium systems in the presence of citrates. Specifically, approaches involving redox reactions with either VCl_3 or nonredox reactions involving V_2O_5 with citric acid led in an aptly efficient fashion to **1**, upon reaction with hydrogen peroxide, at appropriately adjusted solution pH values.

Complex **1** belongs to the general structural family of vanadium(V)−peroxo−citrate complexes, which include species **3** and **5**. Structural comparisons with complex $(NH_4)_2[V^V_2O_2(O_2)_2(C_6H_6O_7)_2]\cdot 2H_2O$ (**3**) and $K_2[V_2O_2(O_2)_2(C_6H_6O_7)_2]\cdot 2H_2O$ (**5**) revealed striking similarities emphasizing the nature of the $[V^V_2O_2]$ core unit, and differences in the citrate mode of coordination and most importantly in the state of protonation of bound citrates as a function of pH (from ~3.5 (**3**) to ~6.5 (**1**)). From such comparisons, the following were evident: (1) The single most important component in both dinuclear peroxo complexes was the $[V^V_2O_2]$ unit, the integrity of which was independent of the pH at which the complexes were synthesized and isolated. In both cases, the core was planar with essentially identical V−O bond distances and O−V−O as well as V−O−V angles. (2) The peroxo moieties were bound to the vanadium ions in the same side-on fashion. (3) The oxidation state of the vanadium ions in the cores of the two complexes was +5. The striking differences between the two species included the following: (a) The protonation states of the bound citrates around the $[V^V_2O_2]$ core of **1** and **3** were different. Regardless of the protonation state of the citrate ligand attached to the core, the terminal carboxylate group not participating in the coordination sphere around vanadium is the molecular locus of protonation in the molecule. (b) The mode of coordination of the citrate ligand around the core unit was different in **1** and **3**. (c) The geometry around the vanadium ions was different. Specifically, the coordination geometry around V(V) in **1** was pentagonal bipyramidal in contrast to the coordination geometry of V(V) ion in **3**, which was pentagonal pyramidal. The aforementioned structural features emphasized the distinct nature of the two species, which was proven by solid state and solution ^{13}C NMR spectroscopy. In both **1** and **3**, the existence of hydrogen-bonding networks was crucial in stabilizing the respective lattices. In particular in complex **1**, the fully deprotonated citrates are responsible for the presence of discrete anions in the lattice that are hydrogen-bonded through the ammonium counterions and lattice water molecules. In contrast, in complex **3**, the anions are hydrogen bonded through the protonated terminal carboxylate groups, thus forming 2D layers parallel to the *ac* diagonal plane. This is a striking feature of the observed lattices in **1** and **3**, rendering them distinct species in the solid state. Similar hydrogen-bonding networks were previously reported in other vanadium−citrate and vanadium−carboxylate complexes.[14−16,21,34]

Of the most important conclusions of the present work was the pH-dependent association of the two dinuclear complexes $(NH_4)_6[V^V_2O_2(O_2)_2(C_6H_4O_7)]_2\cdot 4.5\ H_2O$ (**1**) and $(NH_4)_2[V^V_2O_2(O_2)_2(C_6H_6O_7)_2]\cdot 2H_2O$ (**3**). Given the fact that the syntheses and isolation of the two complexes were pursued at pH values ranging from 3.5 (**3**) to 6.5 (**1**), it logically ensued that a potential association among the two species might be in place in aqueous solutions. Key to this supposition was the fact that a previous pH-dependence had been noted between the non-peroxo congener complexes $[V^V_2O_4(C_6H_6O_7)]_2^{2-}$ [16,20] and $[V^V_2O_4(C_6H_4O_7)]_2^{6-}$,[17,35] with the two species containing bound citrate ligands differing only in their protonation state. The pH-dependent transformations involving the two species further proved the aforementioned point (Figure 1). It appears, therefore, that pH dependence is a phenomenon characterizing peroxo and non-peroxo vanadium citrate complexes of similar or identical structures, differing only in the protonation state of the

(34) Burojevic, S.; Shweky, I.; Bino, A.; Summers, D. A.; Thompson, R. C. *Inorg. Chim. Acta* **1996**, *251*, 75−79.
(35) Zhou, Z.-H.; Wan, H.-L.; Hu, S.-Z.; Tsai, K.-R. *Inorg. Chim. Acta* **1995**, *237*, 193−197.

coordinated citrate ligands around their respective basic core units. It further attests to the notion that the involved species participate as components in the speciation schemes containing vanadium in the presence of citrate.

The observed protonation−deprotonation of the citrate ligands bound to the $V^V_2O_2$ core in each complex bears relevance to a similar protonation−deprotonation process purported to involve (a) the R-homocitrate ligand attached to the inorganic FeMoco cofactor of the nitrogenase enzyme and (b) the citrate ligand of the heterometallic cofactor in the $NifV^-$ nitrogenase enzymes.[36]

Interconversions. The acid−base reactivity associating **1** and **3** emphasizes the stability of the basic $V^V_2O_2$ core, in the investigated pH range from 3.5 to 7.5, as a scaffold around which proton-coupled chemical events take place. The ramifications of such chemistry at the biological level may be profound, (a) relating protonation−deprotonation with biochemical events in molecular targets abutting vanadium(V) ions and (b) reflecting site specificity in protonation−deprotonation events linked with V(V).

In the case of the transformation of complex **1** to complex **2**, which is the non-peroxo congener species, it appears that the peroxo group departs from the initial V_2O_2 scaffold even under the influence of stirring at room temperature over a period of 24 h. This is consistent with the UV−vis behavior of **1** as a function of time (vide supra). The event signifies the extent of stability of that particular vanadium−peroxo−citrate complex in aqueous solutions. Concurrently, it provides an explanation into the sequence of events unfolding upon thermal transformation of complex **1**. As a matter of fact, in a logical follow-up exploration of the reactivity of complex **1**, heating of the requisite solutions resulted in the transformation of **1** to complex $[V^{IV}_2O_2(C_6H_4O_7)_2]^{4-}$ (**4**), a species that had been previously characterized spectroscopically and crystallographically.[15] Bearing in mind that the thermal transformation of complex **2** had been studied in the past and had been shown to yield complex **4**, it appears that at least one important piece of information on the mechanistic path leading stepwise from **1** to **4** had been provided through the investigated transformations between pairs of **1**, **2**, and **4**. The peroxide group departs early on in the conversion process, followed by the chemical conversion of the intermediate **2** to **4**.[37] The reverse process of peroxide addition to the non-peroxo species **2** was also expediently shown to proceed in the presence of excess hydrogen peroxide, leading to complex **1**. Thus, a fully accounted for process of interconversion between **1** and **2** was clarified, associating the two species with the vanadium(IV)-containing species **4**. Further connection between **4** and **3** has been reported in the past.[37]

An equally important observation in the discovery of the connection between **1** and **4** is that the end-product of the requisite thermal transformation is a complex (**4**), which contains vanadium in the oxidation state +4, while the original complex **1** contains vanadium in the oxidation state +5. Thus, a redox reaction takes place, resulting in the reduction of each vanadium in the $V^V_2O_2$ core by one electron. This particular chemical behavior had been noted in the past during the exploration of similar transformations between pairs of non-peroxo− as well as peroxo−vanadium−citrate dinuclear species.[37] It was then shown that, during thermal transformations, one vanadium-bound citrate acts as the target of the oxidative activity of vanadium(V), as a result of which the former is decarboxylated to give acetone dicarboxylate and carbon dioxide in a two electron process. This oxidative decarboxylation of citrate in the presence of an oxidatively competent metal ion had been reported to occur in the past for a number of carboxylic acids.[31d,38,39] To this end, one vanadium(V) dinuclear species **1** is reduced by the arising electrons, producing the $V^{IV}_2O_2$ core containing vanadium(IV). The reaction affords the reduced product $[V^{IV}_2O_2(C_6H_4O_7)_2]^{4-}$, acetone dicarboxylate, carbon dioxide, and a remaining transformed vanadium(V) species such as $[V^V_2O_5(C_6H_4O_7)(H_2O)_2]^{4-}$. The proposal for the latter vanadium(V) species was consistent with (a) reports on aqueous speciation of the vanadium(V)−citrate system containing similar species in the same pH range[13c] and (b) prior findings from our work supporting the existence of fully deprotonated citrate ligand(s) coordinated to vanadium(V).[17] In an alternative and equally probable process, the components $H_2VO_4^-$, $C_6H_5O_7^{3-}$, and OH^- could also reflect products of the proposed "decomposed" species $[V^V_2O_5(C_6H_4O_7)(H_2O)_2]^{4-}$ in an overall reaction scheme, which is proposed here.

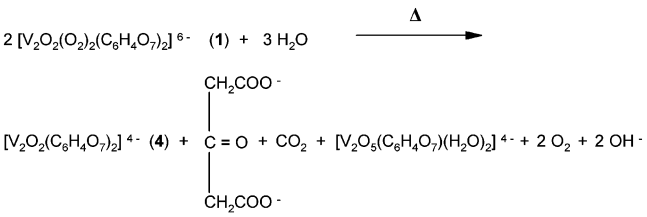

In view of the complexity of this reaction, other products may also form that currently elude identification. To this end, details of the reaction are in further need of perusal. Collectively, both acid−base and thermal transformations provided significant insight into (a) the linkage of vanadium−peroxo−citrate complexes as viable partners of the corresponding speciation scheme and (b) the relations of diverse vanadium−citrate species, at different oxidation levels of vanadium, in aqueous media.

(36) (a) Smith, B. E.; Durrant, M. C.; Faihurst, S. A.; Gormal, C. A.; Grönberg, K. L. C.; Henderson, R. A.; Ibrahim, S. K.; Le Gall, T.; Pickett, C. J. *Coord. Chem. Rev.* **1999**, *185*−*186*, 669−687. (b) Grönberg, K. L. C.; Gormal, C. A.; Durrant, M. C.; Smith, B. E.; Henderson, R. A. *J. Am. Chem. Soc.* **1998**, *120*, 10613−10621. (c) Howard, J. B.; Rees, D. C. *Chem. Rev.* **1996**, *96*, 2965−2982.

(37) Kaliva, M.; Kyriakakis, E.; Raptopoulou, C. P.; Terzis, A.; Salifoglou, A. *Inorg. Chem.* **2002**, *41*, 7015−7023.

(38) (a) Urzúa, U.; Kersten, P. J.; Vicuña, R. *Arch. Biochem. Biophys.* **1998**, *360*, 215−222. (b) Mukhopadhyay, S.; Chaudhury, S.; Das, R.; Banerjee, R. *Can. J. Chem.* **1993**, *71*, 2155−2159. (c) Datta, S. P.; Grzybowski, A. K.; Tate, S. S. *Nature* **1965**, 1047−1049. (d) Li, X.; Pecoraro, V. L. *Inorg. Chem.* **1989**, *28*, 3403−3410. (e) Friedman, T. E.; Haugen, G. E. *J. Biol. Chem.* **1943**, *147*, 415−441.

(39) (a) Jones, J. R.; Waters, W. A.; Littler, J. S. *J. Chem. Soc.* **1961**, 630−633. (b) Meier, I. K.; Schwartz, J. *J. Org. Chem.* **1990**, *55*, 5619−5624.

Table 4. FT-IR Frequencies and V−O Distances for Peroxo and Non-Peroxo Vanadium(V)−(α-hydroxy)carboxylate Complexes Synthesized and Isolated under Similar pH Conditions

pH	compd	$\nu_{as}(COO^-)$ (cm^{-1})	$\nu_s(COO^-)$ (cm^{-1})	V−O distance (Å)	coordination geometry	state of ligand deprotonation
6.5	$(NH_4)_6[V_2O_2(O_2)_2(C_6H_4O_7)_2]\cdot 4.5H_2O$ (**1**)[a]	1631−1569	1399	2.322(2)	pentagonal bipyramid	full
3.5	$(NH_4)_2[V_2O_2(O_2)_2(C_6H_6O_7)_2]\cdot 2H_2O$ (**3**)[b]	1676−1610	1417	2.496(2)	pentagonal pyramid	double
7.0	$(NH_4)_4[V_2O_2(O_2)_2(C_4H_3O_5)_2]\cdot 3H_2O$ (**6**)[c]	1639−1565	1421−1380	2.294(3)	pentagonal bipyramid	full
4.5	$K_2[V_2O_2(O_2)_2(C_4H_4O_5)_2]\cdot 2H_2O$ (**8**)[c]	1675−1577	1448−1384	2.482(2)	pentagonal pyramid	double
7.5	$(NH_4)_6[V_2O_4(C_6H_4O_7)_2]\cdot 6H_2O$ (**9**)[d]	1640−1570	1400		intermediate between trigonal bipyramid and square pyramid ($\tau = 0.32$)	full
3.5	$(NH_4)_2[V_2O_4(C_6H_6O_7)_2]\cdot 2H_2O$[b]	1732,1700−1626	1402		intermediate between trigonal bipyramid and square pyramid ($\tau = 0.32$)	double

[a] This work, $(C_6H_4O_7)^{4-}$ = citrate. [b] $(C_6H_6O_7)^{2-}$ = citrate.[14d,16] [c] $(C_4H_3O_5)^{3-}$ = malate, $(C_4H_4O_5)^{2-}$ = malate.[21] [d] $(C_6H_4O_7)^{4-}$ = citrate.[17]

Spectroscopic and Structural Correlations in Peroxo- and Non-Peroxo-Containing Vanadium−(α-hydroxy)carboxylate Complexes. The advent of synthetic and structural chemistry in the vanadium−peroxo−(α-hydroxy)carboxylate field has afforded several species,[14d,16,21] for which specific trends emerge between spectroscopic and structural characteristics (Table 4). In particular, as the pH, at which the synthesis and isolation of the peroxo−citrate and peroxo-malate complexes takes place, decreases, (a) the frequencies for the $\nu_{as}(COO^-)$ and $\nu_s(COO^-)$ stretches of the carboxylate carbonyls shift to higher values, yet still lower than the ones of the free ligands, (b) the coordination geometry changes consistently from pentagonal bipyramidal to pentagonal pyramidal around the vanadium ions of the $V^V_2O_2$ core, and (c) in congruence with the observed geometry around vanadium(V), the V−O distance (V···O(7) (**1**) 2.322(2) Å and V···O(1) (**3**) 2.496(2) Å in Figure 1) from the vanadium center to the terminal carboxylate oxygen axially trans to the doubly bonded oxygen increases, reflecting the protonation of the corresponding carboxylate group and the decrease in the charge of the assembled complex anion (**3**). In the case of the non-peroxo congener complexes bearing citrate ligands, the observed trends are similar to those in the peroxo analogues.

What is striking between the two families of complexes (peroxo and non-peroxo) is that (a) in the case of the peroxo species, the observed trends are linked to changes in the coordination sphere and geometry around the vanadium centers of the V_2O_2 core, and (b) in the case of the non-peroxo complexes, the observed geometry is different from that in the peroxo species, and it remains insensitive to the FT-IR frequency shift trends.

As the body of structurally and spectroscopically characterized vanadium−(α-hydroxy)carboxylate complexes rises in numbers, further information is expected to shed light into the observed spectroscopic and structural trends. Collectively, these trends may relate to the chemical behavior in variable pH aqueous media and to the potential biological activity of related vanadium species arising in biological fluids.

Aqueous Vanadium(V)−Peroxo−Citrate Speciation. Solution speciation studies in the past have proposed the existence of a stable V_2O_2 core containing species between vanadium(V) and citrate (albeit not identical with the complexes known and characterized today).[13c] The aqueous vanadium chemistry advances to date have shown that the $V^V_2O_2$ core, in all synthetic dinuclear vanadium(V)−citrate complexes, stays intact, with pH acting as a molecular switch, dictating the nature of species in aqueous vanadium distributions in the presence of citrate and hydrogen peroxide. Consequently, in the hydrogen peroxide chemistry of the vanadium−citrate system, structural changes occurring as a result of pH variation of the medium, in which complex formation and isolation occurs, project potential events unfolding in the speciation schemes of the requisite system(s).

It is known that vanadium interacts with a variety of biological targets bearing diverse structural attributes. Logically then, these interactions are tightly linked with both the solubility and bioavailability of the various forms of vanadium presented to the interacting biological targets. In turn, the associated chemical, structural, and spectroscopic properties of the vanadium species of interest are of great importance as they in fact reflect the ultimate chemical and biological activity of vanadium. In this sense, the aforementioned properties on the ternary vanadium peroxo−citrate complex(es) discussed herein, namely complex **1** and its congener low pH complex **3**, formulate the basis on which potential (bio)chemical reactivity might arise in aqueous media. It should be noted that vanadium−peroxo species have been known to exert biological reactivity on variable biological targets at various pathophysiological aberrations in humans (insulin mimesis, antitumorigenesis, etc.).[5−10]

Undoubtedly, the new ternary V(V)−peroxo−citrate species $[V^V_2O_2(O_2)_2(C_6H_4O_7)_2]^{6-}$ (**1**), close to the physiological pH value, provides a new impetus into the pursuit of analogous species partaking of the distribution of vanadium(V) in the presence of the two physiological ligands and affording the possibility for further biological action. In view of the fact that presently two structural partners (**1** and **3**) are shown to be components of the speciation of the vanadium−peroxo−citrate ternary system, more in-depth work is needed to (a) unravel new species, linked to the particular vanadium system, bearing distinct chemical and structural properties and (b) characterize fully the distribution of possible species arising as a result of the presence of the aforementioned constituents in this ternary system. Extraction of pertinent information on the vanadium(V)−peroxo−citrate ternary system speciation is currently not available and should be pursued. Collectively, gaining new knowledge on well-defined, well-characterized, and pH-linked complexes

of vanadium with peroxide and citrate, through structural speciation, stands promising in further assessing complex (bio)chemical interactions between vanadium with biological partners. On this basis, species such as complex **1** represent just a single paradigm arising from a long effort in this direction and reflect the potential (bio)chemical diversity of the general vanadium−peroxo−(α-hydroxy)carboxylate system. Research into this area of biological importance is currently ongoing in our labs.

Acknowledgment. Funding of this research by EPEAEKII, Heraklitos Grant, Greece, is gratefully acknowledged.

Supporting Information Available: X-ray crystal crystallographic files, in CIF format, and listings of positional and thermal parameters and H-bond distances and angles for **1**. This material is available free of charge via the Internet at http://pubs.acs.org.

IC034283I